B J H 8 1 4 4 B
Journal Name Manuscript No.
Dispatch: 2.3.10 Journal: BJH CE: Varun Kumar
Author Received: No. of pages: 10 PE: Subhashree
bjh research paper

Pharmacodynamic and efficacy studies of the novel proteasome inhibitor NPI-0052 (marizomib) in a human plasmacytoma xenograft murine model

Ajita V. Singh,[1] Michael A. Palladino,[2] G. Kenneth Lloyd,[2] Barbara Potts,[2] Dharminder Chauhan[1]* and Kenneth C. Anderson[1]*

[1]The LeBow Institute for Myeloma Therapeutics and Jerome Lipper Myeloma Center, Department of Medical Oncology, Dana Farber Cancer Institute, Harvard Medical School, Boston, MA, and [2]Nereus Pharmaceuticals, San Diego, CA, USA

Received 18 November 2009; accepted for publication 28 January 2010

Correspondence: Kenneth C. Anderson, MD and Dharminder Chauhan, PhD, Dana-Farber Cancer Institute, Mayer Building Room 561, 44 Binney Street, Boston, MA 02115, USA.
E-mail: Kenneth_Anderson@dfci.harvard.edu; Dharminder_Chauhan@dfci.harvard.edu
*Contributed equally as senior authors.

Summary

Our previous study showed that the novel proteasome inhibitor NPI-0052 induces apoptosis in multiple myeloma (MM) cells resistant to conventional and bortezomib (Velcade^{TM}) therapies. *In vivo* studies using human MM-xenografts demonstrated that NPI-0052 is well tolerated, prolongs survival, and reduces tumour recurrence. These preclinical studies provided the basis for an ongoing phase-1 clinical trial of NPI-0052 in relapsed/refractory MM patients. Here we performed pharmacodynamic (PD) studies of NPI-0052 using human MM xenograft murine model. Our results showed that NPI-0052: (i) rapidly left the vascular compartment in an active form after intravenous (i.v.) administration, (ii) inhibited 20S proteasome chymotrypsin-like (CT-L, β5), trypsin-like (T-L, β2), and caspase-like (C-L, β1) activities in extravascular tumours, packed whole blood (PWB), lung, liver, spleen, and kidney, but not brain and (iii) triggered a more sustained (>24 h) proteasome inhibition in tumours and PWB than in other organs (<24 h). Tissue distribution analysis of radiolabeled compound (^{3}H-NPI-0052) in mice demonstrated that NPI-0052 left the vascular space and entered organs as the parent compound. Importantly, treatment of MM.1S-bearing mice with NPI-0052 showed reduced tumour growth without significant toxicity, which was associated with prolonged inhibition of proteasome activity in tumours and PWB but not normal tissues.

Keywords: multiple myeloma, pharmacology, apoptosis.

Protein degradation regulates normal cellular homeostasis through a multi-subunit complex called the proteasome (Goldberg, 2003; Adams, 2004). Pioneering studies by another group showed that ATP-dependent conjugation of proteins with polypeptide (ubiquitin) mediated protein degradation (Ciehanover *et al*, 1978; Ciechanover *et al*, 1980a,b, 1984; Hershko *et al*, 1980). The 26S proteasome complex (Wilk & Orlowski, 1983; Hough *et al*, 1987; Waxman *et al*, 1987) consists of 19S units and a 20S proteasome core (Arrigo *et al*, 1988; Ganoth *et al*, 1988); the 19S units regulate entry of ubiquitinated proteins into the 20S core chamber (Peters *et al*, 1994; Goldberg, 2003). Protein ubiquitination occurs *via* ATP-dependent complex enzymatic reactions involving E1 and E2 ubiquitin enzymes, as well as E3 ubiquitin ligases. Recognition of ubiquitinated proteins by the 19S regulatory subunits allows for entry and degradation of proteins into small peptides of 4–20 amino acids. Proteasomal activities residing within the 20S core complex i.e., chymotrypsin-like (CT-L, β5), trypsin-like (T-L, β2), and caspase-like (C-L, β1), are responsible for protein degradation(Arendt & Hochstrasser, 1997). Importantly, to date, many human diseases have been linked to defects in the ubiquitin-proteasome signalling (UPS) pathway (Adams, 2004), suggesting the clinical utility of targeting proteasomes.

Our preclinical and clinical studies provided the basis for the US Federal Drug Administration approval of the first in class proteasome inhibitor bortezomib (Velcade^{TM}), for the treatment of relapsed/refractory, relapsed, and newly diagnosed MM (Hideshima *et al*, 2001; Kane *et al*, 2003; Richardson *et al*, 2003, 2005; Adams, 2004; San Miguel *et al*, 2008). As with other agents, however, dose-limiting toxicities and the development of resistance limits its long-term utility (Lonial *et al*, 2005; Richardson *et al*, 2006, 2007). Our recent study demonstrated that a novel proteasome inhibitor NPI-0052 (Feling *et al*, 2003) (USAN name marizomib) is distinct from bortezomib; and triggers apoptosis in MM cells resistant to

bortezomib therapies (Chauhan *et al*, 2005). These preclinical data provided the basis for an ongoing phase-1 clinical trial of NPI-0052 in relapsed/refractory MM patients.

In the present study, we utilized our human MM xenograft mouse model to define the distribution profile of NPI-0052 in various tissues and tumour, and in parallel analysed the kinetics of proteasome inhibition. Our data showed that NPI-0052 rapidly distributed from the vascular compartment into tumour and organs, associated with both prolonged proteasome inhibition in tumours and PWB and a marked delay in tumour growth.

3 Material and methods

Cell culture

Human MM.1S MM cells were kindly provided by Dr Steven Rosen (Northwestern University, Chicago, IL, USA), and grown in RPMI-1640 media supplemented with 10% heat-inactivated fetal-bovine serum, 100 units/ml penicillin, 100 μg/ml streptomycin, 2 mmol/l L-glutamine, and plasmocin^{TM} (10 μg/ml), as previously described (Chauhan *et al*, 2005). Prior to inoculation of MM.1S cells in severe combined immunodeficient (SCID) mice, cell viability was assessed by trypan blue exclusion assay, as previously described(Chauhan *et al*, 2008).

Reagents

NPI-0052 and ^{3}H-NPI-0052 (185 GBq/mmol) were provided by Nereus Pharmaceuticals, Inc. For the efficacy and proteasome inhibition studies in mice, NPI-0052 was dissolved in 100% dimethyl sulphoxide (DMSO) to generate a 10 mg/ml stock solution, aliquoted, and stored frozen at −80°C. For intravenous (i.v.) administration, NPI-0052 was dissolved in 100% DMSO and serially diluted with 5% Solutol (Solutol® HS 15; polyethylene glycol 660 12-hydroxystearate, BASF, Shreveport, LA, USA) to yield a final concentration of 2% DMSO. The vehicle control consisted of 2% DMSO and 98% Solutol (5%). The pH of the dosing solutions was between 6 and 7. Flurogenic proteasome substrates succinyl-Leu-Leu-Val-Tyr-AMC and Z-Leu-Leu-Glu-AMC were obtained from Boston Biochem (Cambridge, MA, USA), and BZ-VGR-AMC from Biomol (Plymouth, PA, USA). Purified 20S proteasome was purchased from Boston Biochem. Culture medium was obtained from Mediatech Inc. (Manassas, VA, USA), and fetal bovine serum (FBS) was purchased from Lonza (Walkersville, MD, USA). Immunoblot analysis was performed using the following primary antibodies: anti-caspase-3, anti-PARP, anti-BIP, anti-pEIF2α, pIkb and anti-Hsp70 (Cell signaling, Beverly, MA, USA); anti-CHOP/GADD153 (Abcam, Cambridge, MA, USA); and anti-GAPDH (BD Bioscience Pharmingen, San Diego, CA, USA). Horseradish peroxidase (HRP)-conjugated secondary antibody (Ab) was purchased from Biosource, and enhanced chemiluminesence kit (ECL) was obtained from Amersham (Arlington Heights, IL, USA).

Human plasmacytoma xenograft model

Animal studies were approved by the DFCI Institutional Animal Care and Use Committee. CB-17 SCID-male mice (4–6 weeks old) were purchased from Charles River Laboratories (Willminghton, MA, USA) and housed for 1–2 weeks before starting experiments. Tumours were established by subcutaneous injection of MM.1S cell line ($5{\cdot}0 \times 10^{6}$ MM.1S cells in 100 ml of serum free RPMI-1640 medium, viability >99%) in the flank region of CB-17 SCID-male mice. The mice were divided into three different groups: Groups 1 and 2 (25 mice per group) for pharmacodynamics (PD) studies (time course) and Group 3 (10 mice) for drug efficacy studies. Tumour size was measured every third day in two dimensions using callipers, and tumour volume was calculated using the formula $V = 0{\cdot}5\ a \times b^{2}$, where a and b are the long and short diameter of the tumour, respectively.

Treatment and dose schedule for PD and efficacy studies

The PD effects of NPI-0052 were assessed by measuring alterations in proteasome activity as a function of increasing exposure times and dose levels of NPI-0052. For the PD studies, mice were treated with vehicle or maximum tolerated dose (MTD) of NPI-0052 (i.v.) when tumours were ∼200–300 mm^{3}. Our prior study (Chauhan *et al*, 2005) established the MTD of NPI-0052 and we have used both single and repeated dosing (three dose) in the present study. For the measurement of proteasome activity, mice were euthanized at 10 min, 1, 4, and 24 h after NPI-0052 dosing. Liver, spleen, lung, kidney, brain and tumour were removed, immediately frozen on dry ice, and subsequently processed for determination of *ex vivo* proteasome activity. PWB was collected into tubes containing heparin from cardiac puncture. For efficacy studies, mice were treated i.v. with vehicle or NPI-0052 (0·15 mg/kg) twice a week for 3 weeks. NPI-0052 was administered *via* the i.v. route at a dose of 0·15 mg/kg either once (D1 for proteasome inhibition), three times (D1, D4, D8 for proteasome inhibition), or six times (D1, D4, D8, D11, D15, D18, for efficacy).

Treatment and dose schedule

For the administration of ^{3}H-NPI-0052 to mice and rats (studies performed under the direction of Nereus at MPI Research, Mattawan, MI, USA), the compound (0·0313 mg, or 185 GBq/ml) was stored at −80°C in 0·1 ml of ethanol. For use the material was formulated to 0·06 mg/ml in 40% propylene glycol/10% ethanol/50% citrate buffer (5 mmol/l final concentration, pH 5·0, stored on ice and used within 5 h of preparation. MM.1S tumour-bearing mice were injected i.v. with ^{3}H-NPI-0052 (0·15 mg/kg; 0·45 mg/m^{2}) (n = 15 mice per group; experiments were performed at MPI Research, Mattawan, MI, USA). Immediately prior to euthanasia, blood was collected from anesthetized mice *via* cardiac puncture following which the mice were euthanized by carbon dioxide inhalation at predetermined time points. Selected organs were

removed, weighed and homogenized (5:1, w/v) in methanol, after which a 10:1 (v/w) ratio of acetonitrile was added to the tissue. This preparation was sonicated for 30 s and subsequently centrifuged at 3000 rpm for 10 min at 4°C. The supernatant was decanted, and formic acid (45%) added to the extracts, frozen at ≤60°C, and then analysed for total radioactivity and NPI-0052 concentrations. Based on the total radioactivity content, the extracts were pooled to obtain a minimum of 15 000 dpm for injection onto the YMC Pro C18 HPLC column. Using the relative retention time for authentic ^{3}H-NPI-0052, the chromatographic peak signal was integrated as a percentage of the total radioactivity chromatographed. Using the specific activity of the dose, the ng-equivalents percentage of ^{3}H-NPI-0052 was calculated. Male Sprague-Dawley rats were administered ^{3}H-NPI-0052 (0·1 mg/kg or 0·6 mg/m^2) by i.v. injection and at predetermined time points (n = 1 per time point) euthanized by deep isoflurane anaesthesia and subsequent submergence in a hexane/dry ice bath for 15 min, then removed and placed on dry ice (experiments performed at MPI Research, Mattawan, MI, USA).

For Quantitative Whole Body Autoradiography (QWBA) (QPS, Newark, DE, USA), the frozen rat carcass was embedded in 2% carboxymethylcellulose, mounted on a microtome stage (Leica CM3600 Crymacrocut) and sections (approximately 40 μm thick) were prepared in the sagittal plane. The sections were placed on Scotch tape, dried, mounted on cardboard, and exposed to a ^{3}H-sensitive phosphor imaging plate (Fuji Biomedical, Stamford, CT, USA) for 7 d in light-tight cassettes, followed by scanning using the Typhoon 9410^{TM} image acquisition system (GE Healthcare, Sunnyvale, CA, USA).

Protein extract preparation

After thawing, tissue samples (liver, lung, brain, kidney, tumour) were homogenized in 1 ml of lysis buffer (0·5 mmol/l EDTA, pH 7·3, 20 mmol/l HEPES, Triton X 100 0·05%) and centrifuged at 14 000 rpm for 30 min at 4°C. Supernatants were collected, and protein concentrations were determined using Bradford assay kit (Pierce, Rockford, IL, USA). Whole blood and splenocytes (obtained after slow mechanical disruption) were first washed with phosphate-buffered saline (PBS); RBCs were then lysed in 5 ml of red blood cell lysis buffer (Sigma, St. Luis, MO, USA) for 5 min at room temperature, followed by washing twice with PBS and lysis in lysis buffer (0·5 mmol/l EDTA, pH 8·0, 20 mmol/l HEPES, Triton X 100 0·05%). Supernatants were collected, and protein concentrations were determined using the Bradford assay kit (Pierce, Rockford, IL, USA).

Proteasome activity assays

20S proteasome activity assays were performed using fluorogenic peptide substrates, as previously described (Lightcap *et al*, 2000; Chauhan *et al*, 2005). 20 μg of protein was used in a total volume of 200 μl for determination of 20S proteasome CT-L, T-L or C-L activity, as described for the *in vitro* 20S proteasome activity assays with these exceptions: (i) the assay buffer consisted of 20 mmol/l HEPES, 0·5 mmol/l EDTA, pH. 8·0, (ii) the substrate used for determination of T-L activity was BZ-VGR-AMC, (iii) the final substrate concentration was 60 μmol/l and (iv) the assay buffer was supplemented with a final concentration of 0·05% sodium dodecyl sulphate (SDS) for the evaluation of CT-L and the C-L activities. Data are presented as % inhibition compared to vehicle control treated animals.

In situ detection of apoptosis, and immunohistochemical (IHC) assessment of microvessel density (MVD)

Apoptotic cells in xenografted MM.1S tumours were identified by IHC staining for caspase-3 activation (Chauhan *et al*, 2008). Microvessel density (MVD), a measure of tumour angiogenesis, was assessed by IHC staining for Factor VIII, as previously described (Chauhan *et al*, 2005, 2008).

Western blotting

Total protein lysates were prepared and immunoblot blot analysis was performed, as previously described (Chauhan *et al*, 2005). Briefly, equal amounts of proteins were resolved by 10% or 12·5% SDS-polyacrylamide gel electrophoresis, and transferred onto nitrocellulose membranes. Filters were blocked by incubation in 5% dry milk in PBST (0·05% Tween-20 in PBS) and probed with anti-Caspase-3, anti-PARP, anti-BIP, anti-pEIF2α, Hsp70, CHOP/GADD153, or anti-GAPDH Abs. Specific immunoreactive bands were detected by staining with HRP-conjugated secondary Abs, and blots were developed by enhanced chemiluminesence (ECL; Amersham, Arlington Heights, IL, USA).

Statistical analysis

Statistical significance of differences observed in untreated mice *versus* mice treated with NPI-0052 for various time periods was determined using a Student's t-test. The minimal level of significance was $P < 0·05$.

Results

Pharmacodynamic (PD) effect of NPI-0052

MM.1S tumour-bearing mice were treated with either a single (D1) or three (D1, D4, and D8) doses of NPI-0052 (0·15 mg/kg, i.v.), and euthanized at 10 min, 1, 4 and 24 h after dosing. PWB, liver, spleen, lung, kidney, brain and tumours were harvested, and analysed for CT-L, C-L, and T-L proteasome activities. Results showed significant inhibition of CT-L, C-L, and T-L proteasome activities in tumours and in these tissues, albeit with differential kinetics (Fig 1). A time course analysis of proteasome activity in response to a single dose treatment of mice showed that: (i) NPI-0052 inhibited all three proteasome

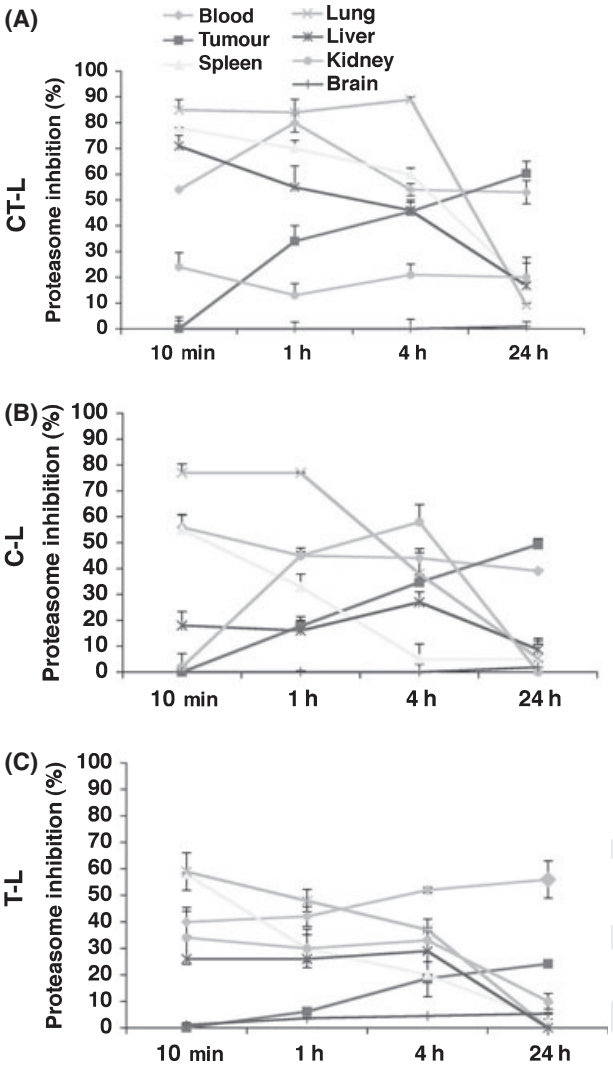

Fig 1. Proteasome inhibition *in vivo* in various tissues and tumours after a single dose of NPI-0052 MM.1S tumour-bearing mice were injected with a single (Day 1) dose of NPI-0052 (0·15 mg/kg, IV); euthanized at 10 min, 1, 4 and 24 h after dosing. PWB, liver, spleen, lung, kidney, brain, and tumour were harvested. Protein extracts were prepared and analysed for CT-L (A), C-L (B), and T-L (C) proteasome activities. Results are presented as percent inhibition compared to vehicle control. Data presented are means ± SD ($n = 3$, $P < 0{\cdot}05$).

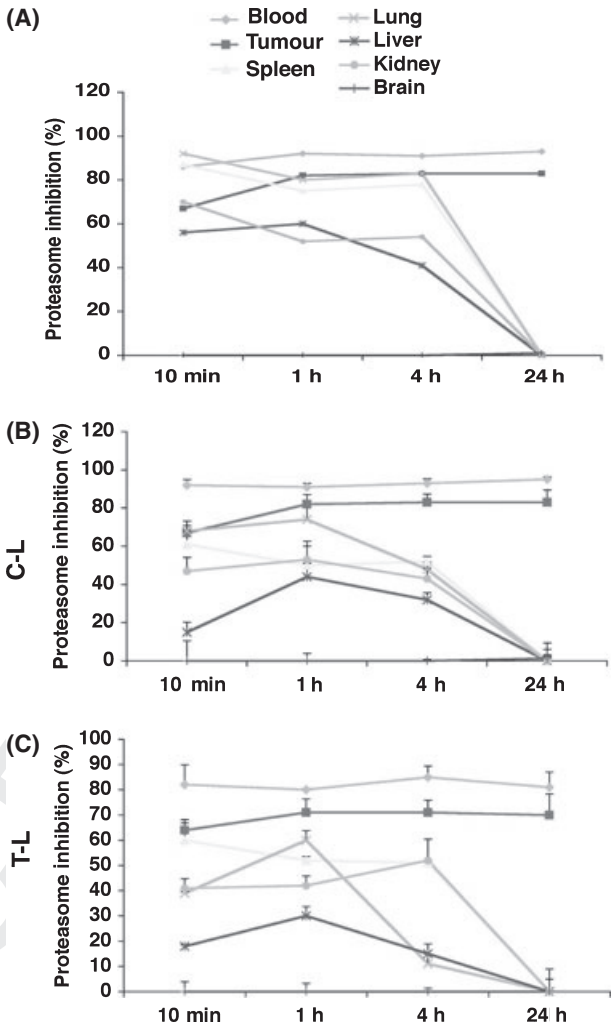

Fig 2. Proteasome inhibition *in vivo* in various tissues and tumours after three doses of NPI-0052. MM.1S tumour-bearing mice were injected with three doses (Day 1, Day 4 and Day 8) of NPI-0052 (0·15 mg/kg, i.v.); euthanized at 10 min, 1, 4 and 24 h after dosing; and PWB, liver, spleen, lung, kidney, brain and tumour were harvested. Protein extracts were prepared and analysed for CT-L (A), C-L (B), and T-L (C) proteasome activities. Results are presented as percent inhibition compared to vehicle control. Data presented are means ± SD ($n = 3$, $P < 0{\cdot}05$).

activities in PWB, liver, spleen, lung, and kidney within 10 min, (ii) inhibition of proteasome activities occurred in tumours by 1 h and was maximal at 24 h, (iii) NPI-0052 did not inhibit proteasome activity in brain tissue and (iv) proteasome activities returned to baseline within 24 h in all tissues examined, except PWB and tumours (Fig 1). These findings demonstrated that NPI-0052 rapidly left the vascular compartments, and targeted liver, spleen, lung, and kidney as early as 10 min. Importantly, NPI-0052-triggered a more sustained inhibition of proteasome activities in tumours and PWB than in other tissues.

We next examined alterations in proteasome activity profiles in various tissues in response to the treatment with three doses of NPI-0052. As seen in Fig 2, our results showed that: (i) all three proteasome activities were significantly inhibited (65–90%) in tumours and PWB, as well as in other tissues except brain within 10 min following the third dose of NPI-0052, (ii) all three proteasome activities in liver, kidney, lung, and spleen recovered within 24 h after treatment with NPI-0052 and (iii) inhibition of CT-L, C-L and T-L activities increased in tumour after the third compared to the first NPI-0052 treatment. For example, all three activities were inhibited approximately 70–80% at 24 h post-third dose vs. 25–60% post single dose. In agreement with our prior studies (Chauhan *et al*, 2005), other normal tissues had the ability to recover proteasome activities even after exposure to three doses of NPI-0052. Importantly, no significant inhibition of proteasome activity

was noted in brain tissue at any time point after either a single or three doses of NPI-0052, suggesting that NPI-0052 does not cross the blood–brain barrier at the efficacious dose tested.

Levels of ^{3}H-NPI-0052 in tumour, blood and kidney of MM.1S-tumour bearing mice

We next examined the distribution of ^{3}H-NPI-0052 in selected organs of MM.1S-tumour bearing mice following the administration of ^{3}H-NPI-0052 (0·15 mg/kg or 0·45 mg/m^{2}; i.v.). The maximal ^{3}H-NPI-0052 levels occurred within 10 min after drug administration in the tumour, and exhibited a similar time-course in the kidney (Fig 3A). The mean drug level observed in the tumour supernatant equated to 2·924 ng/g tumour tissue (8·8 nmol/l), which was greater than the 50% growth inhibitory concentrations of NPI-0052 for MM.1S cells (IC_{50}: 7 nmol/l), as previously reported (Chauhan *et al*, 2005). Our prior study also showed that these concentrations of NPI-0052 markedly blocked all three proteasome activities (Chauhan *et al*, 2005). Importantly, in the present study as well, these drug levels were sufficient to induce anti-tumour activity (Fig 4A) and trigger proteasome inhibition in tumours (Figs 1, 2 and 5A).

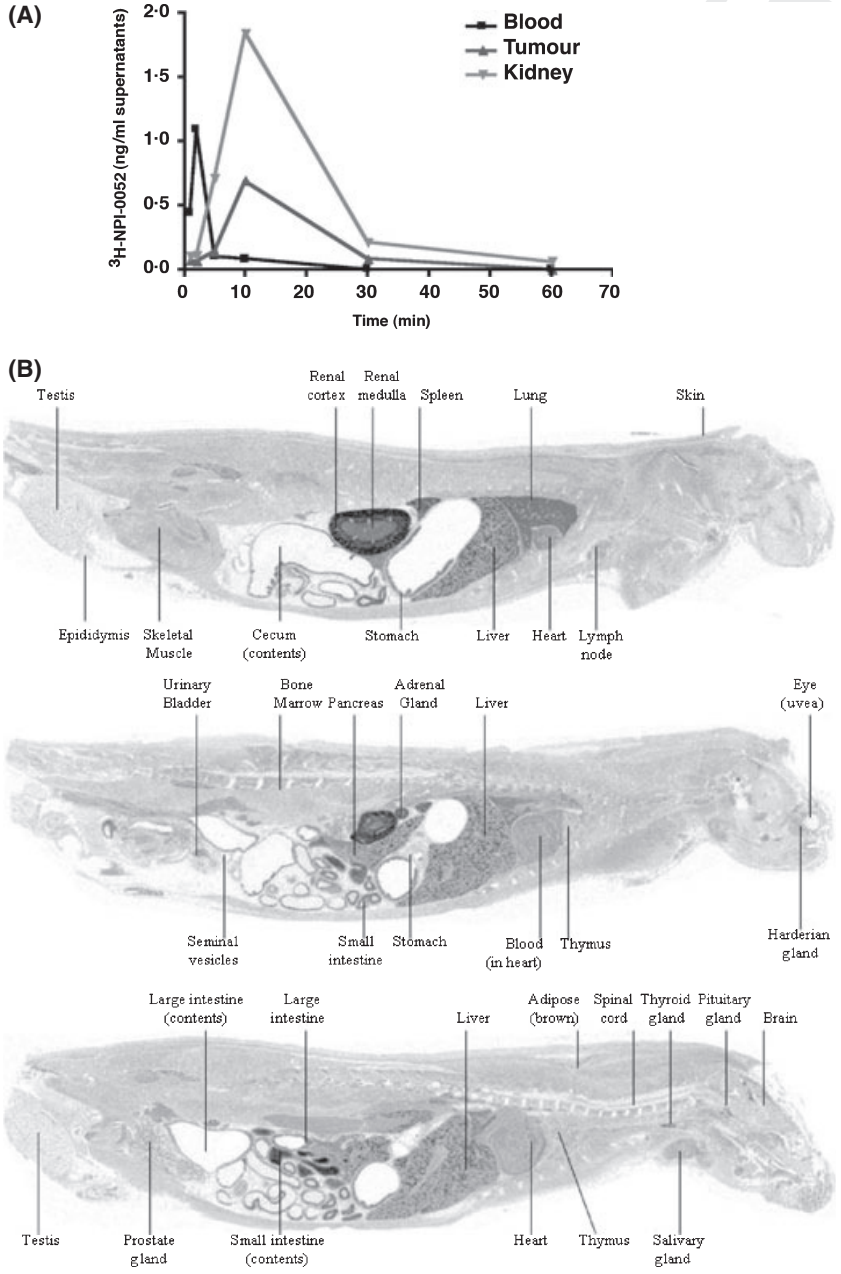

Fig 3. Distribution of radioactivity following i.v. administration of 3H-NPI-0052. (A) Distribution of ^{3}H-NPI-0052 in MM.1S-tumour bearing mice following a single i.v. dose of 0·15 mg/kg. (B) Whole-body autoradiogram of the radioactivity distribution in a male albino rat at 10 min post-dose following a single i.v. administration of [^{3}H]-NPI-0052 at a target dose of 0·1 mg/kg.

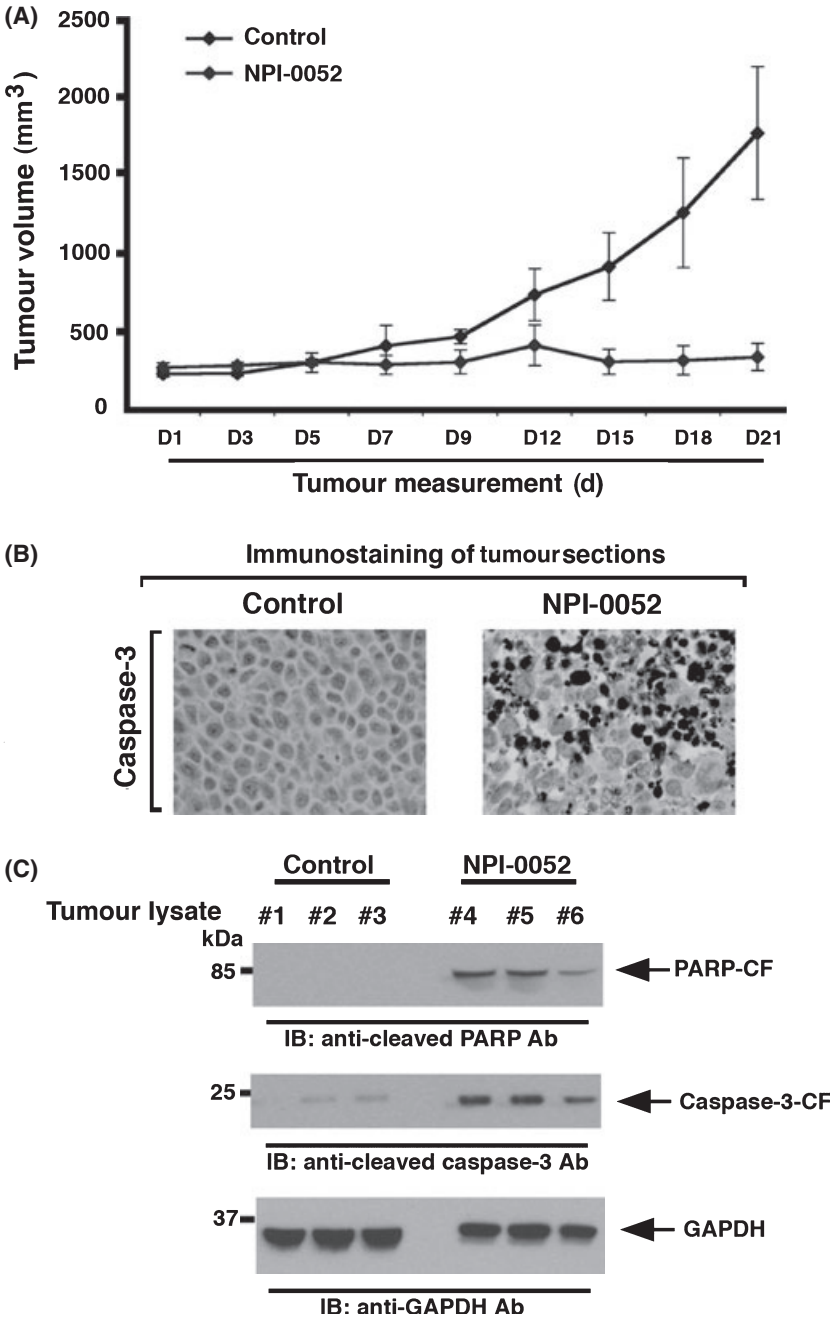

Fig 4. NPI-0052 inhibits human plasmacytoma growth in SCID mice. (A) Mice (n = 5 EA/group) received NPI-0052 (0·15 mg/kg; i.v.) on a twice weekly schedule for 3 weeks; and change in tumour volume was measured on the indicated days. A significant delay in tumour growth was noted in NPI-0052-treated mice compared to vehicle-treated control mice, as early as day 7 ($P < 0·005$). Bars indicate means ± SD. (B) Micrographs show apoptotic cells identified by caspase-3 cleavage (dark brown cells) in tumours harvested on day 21 (endpoint) from untreated- or NPI-0052 (0·15 mg/kg)-treated mice. Photographs are representative of two mice receiving same treatment. Original magnification ×40. (C) Mice were treated with vehicle (control) or NPI-0052 (as in panel A), and tumours were harvested 3 h after the last treatment (Day 21). Protein lysates were prepared and subjected to immunoblot analysis with anti-PARP, anti-cleaved caspase-3, or anti-GAPDH Abs. Immunoblots show analysis of tumour lysates from three mice in each group (vehicle alone 1–3 and NPI-0052-treated mice 4–6).

Distribution of ^{3}H-NPI-0052 in Sprague-Dawley rats

To confirm our findings in MM.1S tumour bearing mice, non-tumour bearing rats were injected with ^{3}H-NPI-0052 (0·1 mg/kg or 0·6 mg/m^2; i.v.), and subjected to QWBA. In agreement with our data using MM.1S-tumour-bearing mice, high levels of ^{3}H-NPI-0052 (total radioactivity) were noted in kidney (Fig 3B). Lung, liver and spleen also

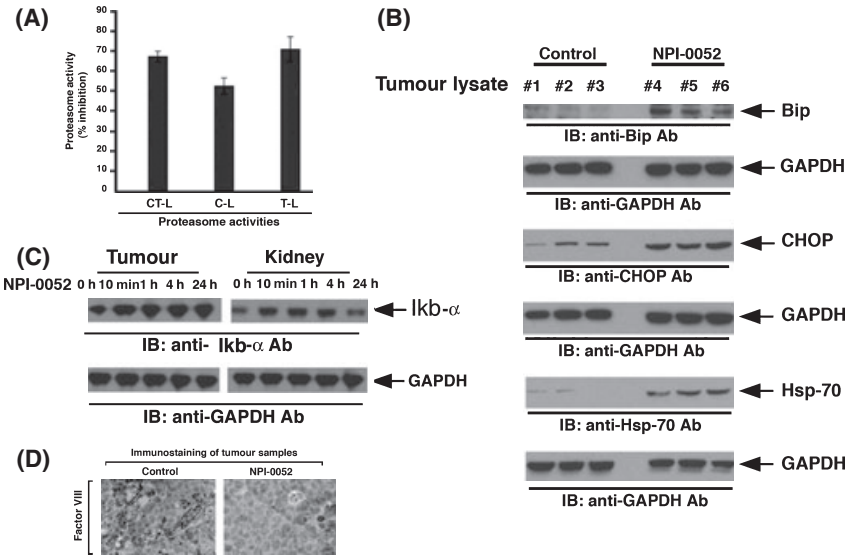

Fig 5. Effect of NPI-0052 on proteasome activities, endoplasmic reticulum stress signalling, and neovascularization, *in vivo* in xenografted MM.1S tumours. (A) Mice bearing MM.1S subcutaneous xenografts were treated with vehicle (control) or NPI-0052 (as in panel A, Fig 4), and tumours were harvested 3 h after the last dose injection (Day 21). Protein lysates were analysed for CT-L, C-L, and T-L proteasome activities. The data represent % inhibition compared to vehicle control-treated animals from two independent experiments. (B) Mice were treated with vehicle (control) or NPI-0052 (as in panel A, Fig 4), and tumours were harvested 3 h after the last dose injection (Day 21). Protein lysates were prepared, and subjected to immunoblot analysis with anti-Bip, anti-CHOP, anti-Hsp70, or anti-GAPDH Abs. Immunoblots show analysis of tumour lysates from 3 mice in each group (vehicle alone 1–3 and NPI-0052-treated mice 4–6). (C) Mice were injected with three doses (Day 1, Day 4 and Day 8) of NPI-0052 (0.15 mg/kg, i.v.); euthanized at 10 min, 1, 4 and 24 h after last dosing; Tumours and kidneys were isolated, protein lysates were prepared and then subjected to immunoblot analysis using IκB or anti-GAPDH Abs. (D) Mice were treated with vehicle (control) or NPI-0052 (as in panel A, Fig 4), and tumours were harvested 3 h after the last dose injection (Day 21). Paraffin-embedded tumour sections were subjected to immunostaining with Factor VIII, a marker for angiogenesis. Micrographs show markedly reduced blood vessel formation in tumour sections from NPI-0052-treated *versus* control mice. Photograph is representative of two mice receiving same treatment. Original magnification ×40.

exhibited relatively high levels, whereas radioactivity was very low/undetectable in the brain, spinal cord and eye.

In vivo anti-MM activity of NPI-0052

Having shown that NPI-0052 targets the proteasome in xenografted tumours, we next determined whether the same dose and schedule of NPI-0052 triggered anti-tumour activity. MM.1S-tumour bearing mice were injected with NPI-0052 (0·15 mg/kg; i.v.) twice a week for 3 weeks, and tumour volume was measured. In agreement with our prior studies (Chauhan *et al*, 2005), NPI-0052 treatment significantly decreased tumour growth relative to untreated vehicle-treated control mice (Fig 4A; $P = 0{\cdot}005$). NPI-0052 treatment was not associated with any toxicity, because no differences in body weight and overall appearance were noted (data not shown). Importantly, the anti-MM activity of NPI-0052 was evident as early as day 5–7, when significant proteasome inhibition was observed in the tumours (Fig 4A).

To determine whether *in vivo* anti-MM activity of NPI-0052 was due to apoptosis, xenografted tumours were harvested from mice, and paraffin-embedded sections were examined for apoptosis by both immunostaining and immunoblot analysis for caspase-3 activation. Tumour sections from NPI-0052-treated mice showed increased numbers of caspase-3 positive cells compared to untreated control mice (Fig 4B). Moreover, immunoblot analysis of tumour lysates confirmed that NPI-0052 triggered caspase-3 cleavage *in vivo* (Fig 4C). Importantly, examination of tumour lysates from NPI-0052-treated mice showed robust cleavage of poly(ADP)-ribose polymerase (PARP), a hallmark of apoptosis (Fig 4C).

Our data therefore showed that either a single or three doses of NPI-0052 inhibited proteasome activity in MM xenografted tumours. For efficacy studies, we utilized a more frequent dosing schedule i.e., twice a week for 3 weeks, and we therefore next questioned whether proteasome activity was similarly affected by this dosing schedule. Tumours excised 3 h after the last dose administration were examined for CT-L, C-L and T-L proteasome activity. Treatment with NPI-0052 (0·15 mg/kg), but not with vehicle alone, significantly inhibited all three proteasome activities (Fig 5A), confirming that NPI-0052-induced anti-MM activity *in vivo* (Fig 4) is associated with inhibition of proteasome activity in tumours.

Prior studies have shown a role for the endothelial reticulum (ER) during bortezomib-induced apoptosis (Mitsiades *et al*, 2002; Landowski *et al*, 2005; Obeng *et al*, 2006; Chauhan *et al*, 2008). Analysis of tumour lysates from NPI-0052-treated mice showed induction of endoplasmaic stress-response, evidenced by upregulation of CHOP/GADD153, phospho-eIF2α, Bip,

and Hsp70, providing *in vivo* evidence of ER stress-related signalling during NPI-0052-triggered cytotoxicity (Fig 5B).

Various prior studies have linked proteasome inhibition with alterations in nuclear factor-kappa B (NF-κB) (Adams *et al*, 1999; Mitsiades *et al*, 2002; Chauhan *et al*, 2005). We next examined whether NPI-0052-triggered proteasome inhibition *in vivo* was associated with changes in NF-κB. Analysis of tumour *versus* normal tissue (kidney) lysates from NPI-0052-treated mice showed stabilization of IκBα levels (Fig 5C). Importantly, the IκBα levels returned to baseline in normal tissue, but not tumours, after 24 h treatment with NPI-0052-the kinetics that correlates with recovery of proteasome activity in normal tissue *versus* tumours (Fig 2). Together, these data provide evidence for a modulation of a proteasome substrate NF-κB by NPI-0052 *in vivo*.

Besides proteasome inhibition and induction of ER-Stress signalling, anti-angiogenic activity of NPI-0052 may also contribute to its anti-MM activity *in vivo*. We therefore next evaluated paraffin-embedded sections of xenografted tumours harvested from NPI-0052-treated and control mice for Factor VIII staining, a marker of angiogenesis. As seen in Fig 5D, NPI-0052 dramatically decreased the number of Factor VIII-positive cells compared to treatment with vehicle alone.

Discussion

Bortezomib (Velcade^{TM}) therapy has proven successful for the treatment of relapsed/refractory, relapsed and newly diagnosed multiple myeloma (MM) (Hideshima *et al*, 2001; Orlowski *et al*, 2002; Richardson *et al*, 2003, 2005; San Miguel *et al*, 2008); however, prolonged treatment can be associated with toxicity and development of drug-resistance (Lonial *et al*, 2005; Richardson *et al*, 2006, 2007). Our recent study showed that the novel proteasome inhibitor NPI-0052 (Feling *et al*, 2003) induces apoptosis in MM cells resistant to conventional and bortezomib therapies (Chauhan *et al*, 2005). The mechanism whereby NPI-0052 overcomes bortezomib-resistance includes the ability to block all three proteasome activities (CT-L, T-L, and C-L) compared to bortezomib, which predominantly inhibits CT-L activity. Additionally, NPI-0052-induced MM cell apoptosis is more dependent on caspase-8- than caspase-9-mediated signalling whereas, bortezomib-triggered cell death requires both caspase-8 and caspase-9 signalling pathways. Importantly, in contrast to bortezomib, NPI-0052-mediated proteasome inhibition is irreversible as evident in PWB but rapidly recovers in normal tissues including PBMC (Chauhan *et al*, 2005). These distinctions between NPI-0052 and bortezomib, in part, may account for the ability of NPI-0052 to overcome bortezomib-resistance. NPI-0052 is orally active (Chauhan *et al*, 2005). In murine tumour model studies, NPI-0052 is well tolerated and prolongs survival, with significantly reduced tumour recurrence. These findings provided the basis for an ongoing phase-1 clinical trial in MM. In the present study, we utilized our human MM xenograft mouse model to study the pharmacodynamic profile of NPI-0052, assessed by alterations in the proteasome activities as well as distribution of ^{3}H-NPI-0052 in various tissues.

We showed that NPI-0052 rapidly distributed from the vascular compartment to various organs and tumours, evident by inhibition of CT-L, C-L, and T-L proteasome activities. These findings are consistent with prior studies (Chauhan *et al*, 2005; Macherla *et al*, 2005) demonstrating the ability of NPI-0052 to target all three 20S proteasome activities. Of note, the kinetics of proteasome inhibition varied between tumours and other tissues. For example, the onset of NPI-0052-induced proteasome inhibition was rapid (within 10 min) in most tissues other than tumour, which occurred at 1 h and was maximal at 24 h. Intravenous injection of either single or three doses of NPI-0052 (0·15 mg/kg) inhibited proteasome activities in peripheral organs, whereas it did not inhibit proteasome activity in the brain, suggesting that NPI-0052 does not cross the blood–brain barrier at this dose and schedule, which is supported by the QWBA study in rats. Analytical studies demonstrated that after i.v. injection, ^{3}H-NPI-0052 rapidly entered the tumour as the parent compound and was present in concentrations consistent with proteasome inhibition and tumour cell death. Following i.v. administration the distribution profile of ^{3}H-NPI-0052 in rats appeared similar to that in MM.1S-tumour bearing mice. Previous studies using bortezomib have also shown rapid clearance and broad tissue distribution in a prostate xenograft tumour model (Adams *et al*, 1999).

Our data show that the duration of proteasome inhibition is more sustained in tumours and PWB (>24 h) than in other tissues. Our prior report showed that a single dose of NPI-0052 (0·15 mg/kg) in rats led to significant proteasome inhibition in PWB, which slowly recovered by Day 7 (Chauhan *et al*, 2005). This may be due to the irreversible covalent binding of NPI-0052 to active proteolytic sites and/or the inability of erythrocytes to generate new proteasomes. Studies using the reversible inhibitor bortezomib showed that proteasome activity recovered after 48 h in blood (Chauhan *et al*, 2005), suggesting that reversible nature of proteasome inhibitor plays a role in proteasome activity recovery in blood.

In tumours, NPI-0052 inhibited all three proteasome activities by 24 h after a single treatment (60% for CT-L; 24% for T-L, and 49% for C-L activity); moreover, administration of three doses enhanced inhibition of proteasome activities by 24 h (83% for CT-L; 70% for C-L; and 70% for T-L). As noted above, sustained inhibition of proteasome activity may be due to the irreversible property of NPI-0052; however, a longer half-life of the proteasome in tumours *versus* normal tissues remains possible. Interestingly, NPI-0052-triggered inhibition of proteasome activity in liver, spleen, kidney, and lungs clearly recovered by 24 h, suggesting that *de novo* and rapid proteasome synthesis may account for the recovery of proteasome activity in these tissues.

Our efficacy studies showed that i.v. injection of 0·15 mg/dose (0·45 mg/m^{2}) given twice weekly for 3 weeks significantly

reduced tumour growth, and was well tolerated. Importantly, this potent *in vivo* anti-MM activity of NPI-0052 was associated with significant inhibition of CT-L, C-L, and T-L proteasome activities (60–80% inhibition), suggesting that frequent dosing of NPI-0052 allows for sustained proteasome inhibition. Furthermore, these *in vivo* findings, coupled with our previously published *in vitro* data showing minimal toxicity of NPI-0052 against normal cells (Chauhan *et al*, 2005), confirm that MM cells are more sensitive to proteasome inhibition than normal cells.

Although the primary target for NPI-0052 is the proteasome, our *in vitro* studies showed that NPI-0052-induced apoptosis in MM cells is associated with loss of mitochondrial membrane potential, increase in O_2^- production, release of cytochrome-c/Smac, and activation of caspases-8, -9 and -3 (Chauhan *et al*, 2005). Biochemical and genetic evidence showed that NPI-0052, in contrast to bortezomib, relies more on the FADD-caspase-8-mediated cell death signalling pathway (Chauhan *et al*, 2005). In agreement with these *in vitro* results, IHC staining of xenografted tumours from NPI-0052-treated mice showed robust PARP cleavage and caspase-3 activation. Importantly, in the present study, we also showed that NPI-0052 upregulated expression of ER-stress related proteins (CHOP/GADD153, phospho-eIF2α, Bip), and Hsp70 in tumours, providing *in vivo* evidence for the role of ER signalling during NPI-0052-triggered cytotoxicity. Finally, results from the Factor VIII immunostaining of tumour sections confirmed the anti-angiogenic activity of NPI-0052 associated with anti-MM activity of NPI-0052 *in vivo*.

Collectively, our findings represent the first attempt to correlate the pharmacodynamic effects of NPI-0052 with its cytotoxic effects against MM *in vivo* in tumour and normal tissues. Importantly, NPI-0052 (i.v.) was well tolerated at the dose and schedule examined. NPI-0052 blockeed all three proteasome activities (CT-L, C-L, and T-L) by >70% in most tissues without significant toxicity. Early results from a phase-1 clinical trial of NPI-0052 in patients with relapsed and relapsed/refractory MM have been reported to demonstrate potential clinical benefit at doses which are well tolerated (Richardson *et al*, 2008). Proteasome inhibition in PWB of treated patients showed a drug-dependent CT-L inhibition, with inhibition up to 28% observed at 0·025 mg/m^2 dose. Complete inhibition of CT-L proteasome activity has been observed at MTD doses (0·7 mg/m^2) in other clinical trials, without evidence of neuropathy or myelosuppression. In MM, dose escalation and scheduling effects are currently ongoing to define the dose-limiting toxicity and MTD, and in order to define a recommended phase-2 dose (RP2D) for evaluation in patients with advanced MM.

Acknowledgements

This investigation was supported by NIH grants SPORE-P50100707, PO1-CA078378, and RO1CA050947; and The LeBow Family Fund to Cure Myeloma.

Authors' contributions

DC designed research, analysed data, and wrote the manuscript; AVS designed research, performed experiments and interpreted data; MP and KL provided H^3-NPI-0052 and QWBA study data, and KCA analysed data and wrote the manuscript.

Disclosure of conflicts of interest

MP, GKL, and BP: Employees of Nereus Pharmaceuticals, Inc. DC and KC: Consultant to Nereus Pharmaceuticals, Inc.

References

Adams, J. (2004) The proteasome: a suitable antineoplastic target. *Nature Reviews. Cancer*, **4,** 349–360.

Adams, J., Palombella, V.J., Sausville, E.A., Johnson, J., Destree, A., Lazarus, D.D., Maas, J., Pien, C.S., Prakash, S. & Elliott, P.J. (1999) Proteasome inhibitors: a novel class of potent and effective antitumor agents. *Cancer Research*, **59,** 2615–2622.

Arendt, C. & Hochstrasser, M. (1997) Identification of the yeast 20S proteasome catalytic centers and subunit interactions required for active-site formation. *Proceedings of the National Academy of Sciences of the United States of America*, **94,** 7156–7161.

Arrigo, A.P., Tanaka, K., Goldberg, A.L. & Welch, W.J. (1988) Identity of the 19S 'prosome' particle with the large multifunctional protease complex of mammalian cells (the proteasome). *Nature*, **331,** 192–194.

Chauhan, D., Catley, L., Li, G., Podar, K., Hideshima, T., Velankar, M., Mitsiades, C., Mitsiades, N., Yasui, H., Letai, A., Ovaa, H., Berkers, C., Nicholson, B., Chao, T.H., Neuteboom, S.T., Richardson, P., Palladino, M.A. & Anderson, K.C. (2005) A novel orally active proteasome inhibitor induces apoptosis in multiple myeloma cells with mechanisms distinct from Bortezomib. *Cancer Cell*, **8,** 407–419.

Chauhan, D., Singh, A., Brahmandam, M., Podar, K., Hideshima, T., Richardson, P., Munshi, N., Palladino, M.A. & Anderson, K.C. (2008) Combination of proteasome inhibitors bortezomib and NPI-0052 trigger *in vivo* synergistic cytotoxicity in multiple myeloma. *Blood*, **111,** 1654–1664.

Ciechanover, A., Elias, S., Heller, H., Ferber, S. & Hershko, A. (1980a) Characterization of the heat-stable polypeptide of the ATP-dependent proteolytic system from reticulocytes. *Journal of Biological Chemistry*, **255,** 7525–7528.

Ciechanover, A., Heller, H., Elias, S., Haas, A.L. & Hershko, A. (1980b) ATP-dependent conjugation of reticulocyte proteins with the polypeptide required for protein degradation. *Proceedings of the National Academy of Sciences of the United States of America*, **77,** 1365–1368.

Ciechanover, A., Finley, D. & Varshavsky, A. (1984) The ubiquitin-mediated proteolytic pathway and mechanisms of energy-dependent intracellular protein degradation. *Journal of Cellular Biochemistry*, **24,** 27–53.

Ciehanover, A., Hod, Y. & Hershko, A. (1978) A heat-stable polypeptide component of an ATP-dependent proteolytic system from reticulocytes. *Biochemical and Biophysical Research Communications*, **81,** 1100–1105.

Feling, R.H., Buchanan, G.O., Mincer, T.J., Kauffman, C.A., Jensen, P.R. & Fenical, W. (2003) Salinosporamide A: a highly cytotoxic

proteasome inhibitor from a novel microbial source, a marine bacterium of the new genus salinospora. *Angewandte Chemie (International ed. in English)*, **42,** 355–357.

Ganoth, D., Leshinsky, E., Eytan, E. & Hershko, A. (1988) A multicomponent system that degrades proteins conjugated to ubiquitin. Resolution of factors and evidence for ATP-dependent complex formation. *Journal of Biological Chemistry*, **263,** 12412–12419.

Goldberg, A.L. (2003) Protein degradation and protection against misfolded or damaged proteins. *Nature*, **426,** 895–899.

Hershko, A., Ciechanover, A., Heller, H., Haas, A.L. & Rose, I.A. (1980) Proposed role of ATP in protein breakdown: conjugation of protein with multiple chains of the polypeptide of ATP-dependent proteolysis. *Proceedings of the National Academy of Sciences of the United States of America*, **77,** 1783–1786.

Hideshima, T., Richardson, P., Chauhan, D., Palombella, V.J., Elliott, P.J., Adams, J. & Anderson, K.C. (2001) The proteasome inhibitor PS-341 inhibits growth, induces apoptosis, and overcomes drug resistance in human multiple myeloma cells. *Cancer Research*, **61,** 3071–3076.

Hough, R., Pratt, G. & Rechsteiner, M. (1987) Purification of two high molecular weight proteases from rabbit reticulocyte lysate. *Journal of Biological Chemistry*, **262,** 8303–8313.

Kane, R.C., Bross, P.F., Farrell, A.T. & Pazdur, R. (2003) Velcade: U.S. FDA approval for the treatment of multiple myeloma progressing on prior therapy. *Oncologist*, **8,** 508–513.

Landowski, T.H., Megli, C.J., Nullmeyer, K.D., Lynch, R.M. & Dorr, R.T. (2005) Mitochondrial-mediated disregulation of Ca2+ is a critical determinant of Velcade (PS-341/bortezomib) cytotoxicity in myeloma cell lines. *Cancer Research*, **65,** 3828–3836.

Lightcap, E.S., McCormack, T.A., Pien, C.S., Chau, V., Adams, J. & Elliott, P.J. (2000) Proteasome inhibition measurements: clinical application. *Clinical Chemistry*, **46,** 673–683.

Lonial, S., Waller, E.K., Richardson, P.G., Jagannath, S., Orlowski, R.Z., Giver, C.R., Jaye, D.L., Francis, D., Giusti, S., Torre, C., Barlogie, B., Berenson, J.R., Singhal, S., Schenkein, D.P., Esseltine, D.L., Anderson, J., Xiao, H., Heffner, L.T. & Anderson, K.C. (2005) Risk factors and kinetics of thrombocytopenia associated with bortezomib for relapsed, refractory multiple myeloma. *Blood*, **106,** 3777–3784.

Macherla, V.R., Mitchell, S.S., Manam, R.R., Reed, K.A., Chao, T.H., Nicholson, B., Deyanat-Yazdi, G., Mai, B., Jensen, P.R., Fenical, W.F., Neuteboom, S.T., Lam, K.S., Palladino, M.A. & Potts, B.C. (2005) Structure-activity relationship studies of salinosporamide A (NPI-0052), a novel marine derived proteasome inhibitor. *Journal of Medicinal Chemistry*, **48,** 3684–3687.

Mitsiades, N., Mitsiades, C.S., Poulaki, V., Chauhan, D., Fanourakis, G., Gu, X., Bailey, C., Joseph, M., Libermann, T.A., Treon, S.P., Munshi, N.C., Richardson, P.G., Hideshima, T. & Anderson, K.C. (2002) Molecular sequelae of proteasome inhibition in human multiple myeloma cells. *Proceedings of the National Academy of Sciences of the United States of America*, **99,** 14374–14379.

Obeng, E.A., Carlson, L.M., Gutman, D.M., Harrington, Jr, W.J., Lee, K.P. & Boise, L.H. (2006) Proteasome inhibitors induce a terminal unfolded protein response in multiple myeloma cells. *Blood*, **107,** 4907–4916.

Orlowski, R.Z., Stinchcombe, T.E., Mitchell, B.S., Shea, T.C., Baldwin, A.S., Stahl, S., Adams, J., Esseltine, D.L., Elliott, P.J., Pien, C.S., Guerciolini, R., Anderson, J.K., Depcik-Smith, N.D., Bhagat, R., Lehman, M.J., Novick, S.C., O'Connor, O.A. & Soignet, S.L. (2002) Phase I trial of the proteasome inhibitor PS-341 in patients with refractory hematologic malignancies. *Journal of Clinical Oncology*, **20,** 4420–4427.

Peters, J., Franke, W. & Kleinschmidt, J. (1994) Distinct 19 S and 20 S subcomplexes of the 26 S proteasome and their distribution in the nucleus and the cytoplasm. *Journal of Biological Chemistry*, **269,** 7709–7718.

Richardson, P.G., Barlogie, B., Berenson, J., Singhal, S., Jagannath, S., Irwin, D., Rajkumar, S.V., Srkalovic, G., Alsina, M., Alexanian, R., Siegel, D., Orlowski, R.Z., Kuter, D., Limentani, S.A., Lee, S., Hideshima, T., Esseltine, D.L., Kauffman, M., Adams, J., Schenkein, D.P. & Anderson, K.C. (2003) A phase 2 study of bortezomib in relapsed, refractory myeloma. *New England Journal of Medicine*, **348,** 2609–2617.

Richardson, P.G., Sonneveld, P., Schuster, M.W., Irwin, D., Stadtmauer, E.A., Facon, T., Harousseau, J.L., Ben-Yehuda, D., Lonial, S., Goldschmidt, H., Reece, D., San-Miguel, J.F., Blade, J., Boccadoro, M., Cavenagh, J., Dalton, W.S., Boral, A.L., Esseltine, D.L., Porter, J.B., Schenkein, D. & Anderson, K.C. (2005) Bortezomib or high-dose dexamethasone for relapsed multiple myeloma. *New England Journal of Medicine*, **352,** 2487–2498.

Richardson, P.G., Briemberg, H., Jagannath, S., Wen, P.Y., Barlogie, B., Berenson, J., Singhal, S., Siegel, D.S., Irwin, D., Schuster, M., Srkalovic, G., Alexanian, R., Rajkumar, S.V., Limentani, S., Alsina, M., Orlowski, R.Z., Najarian, K., Esseltine, D., Anderson, K.C. & Amato, A.A. (2006) Frequency, characteristics, and reversibility of peripheral neuropathy during treatment of advanced multiple myeloma with bortezomib. *Journal of Clinical Oncology*, **24,** 3113–3120.

Richardson, P.G., Sonneveld, P., Schuster, M.W., Irwin, D., Stadtmauer, E.A., Facon, T., Harousseau, J.L., Ben-Yehuda, D., Lonial, S., San Miguel, J.F., Cavenagh, J.D. & Anderson, K.C. (2007) Safety and efficacy of bortezomib in high-risk and elderly patients with relapsed multiple myeloma. *British Journal Haematology*, **137,** 429–435.

Richardson, P., Hofmeister, C., Zimmerman, T., Chanan-Khan, A., Spear, M., Palladino, M.A., Longenecker, A., Cropp, G., Lloyd, K.G., Wear, S., Hannah, A.L. & Anderson, K. (2008) Phase 1 Clinical Trial of NPI-0052, a Novel Proteasome Inhibitor in Patients with Multiple Myeloma. *Blood (ASH Annual Meeting Abstracts)*, **2770**.

San Miguel, J.F., Schlag, R., Khuageva, N.K., Dimopoulos, M.A., Shpilberg, O., Kropff, M., Spicka, I., Petrucci, M.T., Palumbo, A., Samoilova, O.S., Dmoszynska, A., Abdulkadyrov, K.M., Schots, R., Jiang, B., Mateos, M.V., Anderson, K.C., Esseltine, D.L., Liu, K., Cakana, A., van de Velde, H. & Richardson, P.G. (2008) Bortezomib plus melphalan and prednisone for initial treatment of multiple myeloma. *New England Journal of Medicine*, **359,** 906–917.

Waxman, L., Fagan, J.M. & Goldberg, A.L. (1987) Demonstration of two distinct high molecular weight proteases in rabbit reticulocytes, one of which degrades ubiquitin conjugates. *Journal of Biological Chemistry*, **262,** 2451–2457.

Wilk, S. & Orlowski, M. (1983) Evidence that pituitary cation-sensitive neutral endopeptidase is a multicatalytic protease complex. *Journal of Neurochemistry*, **40,** 842–849.

Author Query Form

Journal: BJH

Article: 8144

Dear Author,
During the copy-editing of your paper, the following queries arose. Please respond to these by marking up your proofs with the necessary changes/additions. Please write your answers on the query sheet if there is insufficient space on the page proofs. Please write clearly and follow the conventions shown on the attached corrections sheet. If returning the proof by fax do not write too close to the paper's edge. Please remember that illegible mark-ups may delay publication.

Many thanks for your assistance.

Query reference	Query	Remarks
1	AUTHOR: Journal style requires that the first forenames of all authors should be given. Please provide the forename for "G. Kenneth Lloyd".	
2	AUTHOR: Please give manufacturer information for the product "Velcade™": company name, town, state (if USA), and country.	
3	AUTHOR: The heading "Material/subjects and methods" has been changed to "Material and methods" as per Journal style. Please confirm.	
4	AUTHOR: 3000 rpm: please replace this with the correct g value.	
5	AUTHOR: 14 000 rpm: please replace this with the correct g value.	
6	AUTHOR: Figure 3 is of poor quality. Please check required artwork specifications at http://authorservices.wiley.com/submit_illust.asp?site = 1	

USING E-ANNOTATION TOOLS FOR ELECTRONIC PROOF CORRECTION

Required Software

Adobe Acrobat Professional or Acrobat Reader (version 7.0 or above) is required to e-annotate PDFs. Acrobat 8 Reader is a free download: http://www.adobe.com/products/acrobat/readstep2.html

Once you have Acrobat Reader 8 on your PC and open the proof, you will see the Commenting Toolbar (if it does not appear automatically go to Tools>Commenting>Commenting Toolbar). The Commenting Toolbar looks like this:

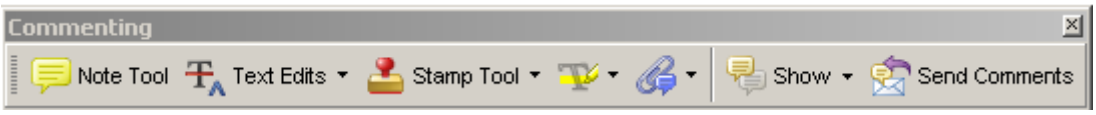

If you experience problems annotating files in Adobe Acrobat Reader 9 then you may need to change a preference setting in order to edit.

In the "Documents" category under "Edit – Preferences", please select the category 'Documents' and change the setting "PDF/A mode:" to "Never".

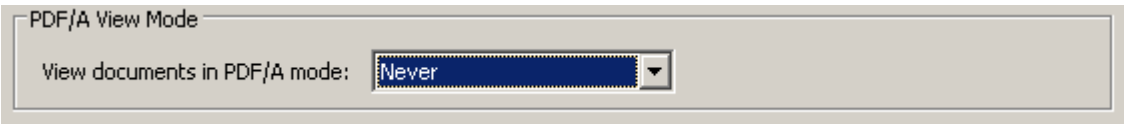

Note Tool — For making notes at specific points in the text

Marks a point on the paper where a note or question needs to be addressed.

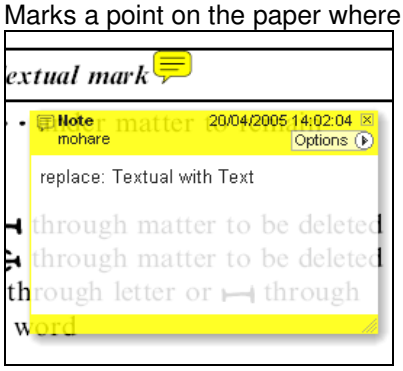

How to use it:

1. Right click into area of either inserted text or relevance to note
2. Select Add Note and a yellow speech bubble symbol and text box will appear
3. Type comment into the text box
4. Click the X in the top right hand corner of the note box to close.

Replacement text tool — For deleting one word/section of text and replacing it

Strikes red line through text and opens up a replacement text box.

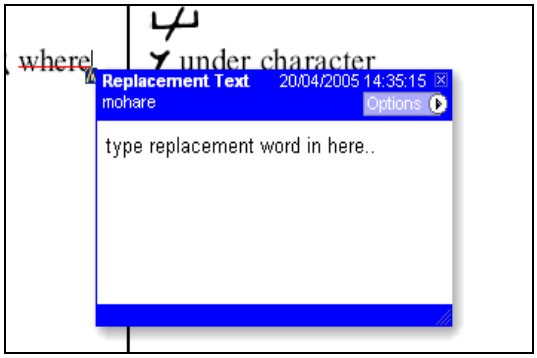

How to use it:

1. Select cursor from toolbar
2. Highlight word or sentence
3. Right click
4. Select Replace Text (Comment) option
5. Type replacement text in blue box
6. Click outside of the blue box to close

Cross out text tool — For deleting text when there is nothing to replace selection

Strikes through text in a red line.

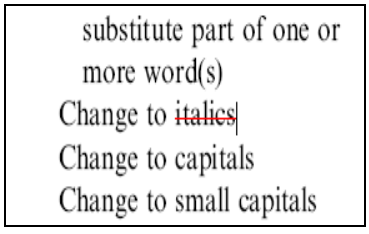

How to use it:

1. Select cursor from toolbar
2. Highlight word or sentence
3. Right click
4. Select Cross Out Text

Approved tool — For approving a proof and that no corrections at all are required.

How to use it:

1. Click on the Stamp Tool in the toolbar
2. Select the Approved rubber stamp from the 'standard business' selection
3. Click on the text where you want to rubber stamp to appear (usually first page)

Highlight tool — For highlighting selection that should be changed to bold or italic.

Highlights text in yellow and opens up a text box.

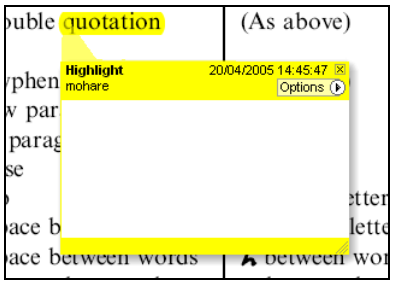

How to use it:

1. Select Highlighter Tool from the commenting toolbar
2. Highlight the desired text
3. Add a note detailing the required change

Attach File Tool — For inserting large amounts of text or replacement figures as a files.

Inserts symbol and speech bubble where a file has been inserted.

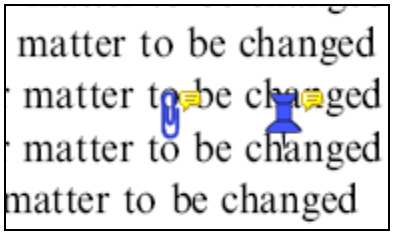

How to use it:

1. Click on paperclip icon in the commenting toolbar
2. Click where you want to insert the attachment
3. Select the saved file from your PC/network
4. Select appearance of icon (paperclip, graph, attachment or tag) and close

Pencil tool — For circling parts of figures or making freeform marks

Creates freeform shapes with a pencil tool. Particularly with graphics within the proof it may be useful to use the Drawing Markups toolbar. These tools allow you to draw circles, lines and comment on these marks.

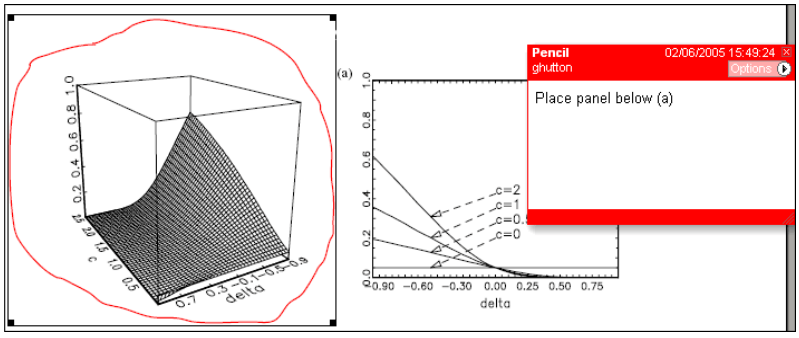

How to use it:

1. Select Tools > Drawing Markups > Pencil Tool
2. Draw with the cursor
3. Multiple pieces of pencil annotation can be grouped together
4. Once finished, move the cursor over the shape until an arrowhead appears and right click
5. Select Open Pop-Up Note and type in a details of required change
6. Click the X in the top right hand corner of the note box to close.

Help

For further information on how to annotate proofs click on the Help button to activate a list of instructions: